The Astrophysical Journal, 845:110 (10pp), 2017 August 20 https://doi.org/10.3847/1538-4357/aa7fea


# On the Age of the TRAPPIST-1 System

Adam J. Burgasser[1] and Eric E. Mamajek[2,3]
[1] Department of Physics, University of California, San Diego, CA 92093, USA
[2] Jet Propulsion Laboratory, California Institute of Technology, 4800 Oak Grove Drive, Pasadena, CA 91109, USA
[3] Department of Physics & Astronomy, University of Rochester, Rochester, NY 14627, USA
*Received 2017 June 1; revised 2017 July 7; accepted 2017 July 12; published 2017 August 17*

## Abstract

The nearby ($d = 12$ pc) M8 dwarf star TRAPPIST-1 (2MASS J23062928−0502285) hosts a compact system of at least seven exoplanets with sizes similar to Earth. Given its importance for testing planet formation and evolution theories, and for assessing the prospects for habitability among Earth-size exoplanets orbiting the most common type of star in the Galaxy, we present a comprehensive assessment of the age of this system. We collate empirical age constraints based on the color-absolute magnitude diagram, average density, lithium absorption, surface gravity features, metallicity, kinematics, rotation, and magnetic activity; and conclude that TRAPPIST-1 is a transitional thin/thick disk star with an age of 7.6 ± 2.2 Gyr. The star's color–magnitude position indicates that it is slightly metal-rich, which is consistent with the previously reported near-infrared spectroscopic metallicity; and it has a radius ($R = 0.121 \pm 0.003\ R_{\odot}$) that is larger by 8%–14% than the predictions of solar-metallicity evolutionary models. We discuss some implications of the old age of this system with regard to the stability and habitability of its planets.

*Key words:* stars: activity – stars: atmospheres – stars: individual (2MASS J23062928-0502285, TRAPPIST-1) – stars: low-mass

## 1. Introduction

TRAPPIST-1 (2MASS J23062928−0502285; Gizis et al. 2000) is an ultracool M8 dwarf 12 pc from the Sun that was recently identified to host at least seven Earth-sized planets, three of which orbit within the star's habitable zone (Gillon et al. 2016, 2017; Luger et al. 2017). The planets were identified by both ground-based and space-based transit observations, and span orbit periods of 1.5–19 days and semimajor axes of 0.011–0.062 au (21–114 stellar radii). These observations and others have provided important constraints on the physical parameters of the star, as summarized in Table 1.

One crucial parameter of TRAPPIST-1 that is currently poorly constrained is its age due to the weak empirical age diagnostics available for ultracool M dwarfs. While rotation (gyrochronology), activity diagnostics, and lithium depletion are standard age-dating tools for solar-type stars (Soderblom 2010), the physical properties of ultracool dwarfs restrict their application at the bottom of the main sequence. The low degree of ionization of ultracool dwarf photospheric gas reduces the star's coupling with magnetic winds, resulting in spin-down timescales that can exceed the age of the Milky Way Galaxy (West et al. 2008). Depletion of lithium, which provides approximate ages for solar-type stars up to 1–2 Gyr (Sestito & Randich 2005), is complete for fully convective low-mass stars by ∼200 Myr, and is only useful for young ultracool dwarfs (Stauffer et al. 1998). Spectral age diagnostics, such as surface gravity-sensitive features, are also limited to stars younger than ∼300 Myr (Allers & Liu 2013). While the kinematics of TRAPPIST-1 suggest that it is an "old disk" star (Leggett 1992; Burgasser et al. 2015), such labels are insufficient to firmly constrain an age. Filippazzo et al. (2015) report a wide age range of 0.5–10 Gyr, while Luger et al. (2017) adopt a more constrained, but still broad, range of 3–8 Gyr. In contrast, several studies in the literature have argued that TRAPPIST-1 may be young based on the strength of its nonthermal magnetic emission (Bourrier et al. 2017; O'Malley-James & Kaltenegger 2017).

Age is necessary for understanding the formation, orbital evolution, stability, and surface evolution (including habitability) of the planets orbiting TRAPPIST-1. Here, we present an analysis of several empirical age diagnostics for this source that allow us to more precisely quantify its age. In Section 2, we analyze in turn the color-absolute magnitude diagram (CMD), average density, lithium abundance, surface gravity features, metallicity, kinematics, rotation, and magnetic activity of the star. In Section 3, we combine these into a concordance age of 7.6 ± 2.2 Gyr, and discuss implications on the stability and habitability of the planetary system.

## 2. Analysis

### 2.1. Age Constraints from the Color-absolute Magnitude Diagram

The locations of TRAPPIST-1 and other late M-type spectral standards and field stars on the $M_{Ks}$ versus $(V - K_s)$ CMD are shown in Figure 1. The comparison data were drawn from Dieterich et al. (2014) and Winters et al. (2015) for nearby M dwarfs with trigonometric parallaxes. A polynomial fit to these data between $3.5 < (V - K_s) < 11.8$ yields

$$\begin{aligned} M_{Ks} = {} & 26.987 - 20.6315(V - K_s) \\ & + 6.88044(V - K_s)^2 - 1.01665(V - K_s)^3 \\ & + 0.0707374(V - K_s)^4 - 0.00188517(V - K_s)^5. \end{aligned} \quad (1)$$

The root mean square scatter is 0.48 mag. Recent spectroscopic surveys of field M dwarfs found median metallicities ranging from [Fe/H] ≃ +0.04 (Newton et al. 2014) to [Fe/H] ≃ −0.03 (Mann et al. 2015), with 1σ dispersions of ∼0.2 dex. Hence, this CMD sequence is largely representative of a solar-metallicity population.

**Table 1**
Stellar Parameters for TRAPPIST-1

| Parameter | Value | Units | References |
|---|---|---|---|
| **Physical Parameters** | | | |
| $\log_{10} L/L_{\rm bol}$ | $-3.28 \pm 0.03$ | dex | 1 |
| $T_{\rm eff}$ | $2560 \pm 50$ | K | 2 |
| [Fe/H] | $+0.04 \pm 0.08$ | dex | 2 |
| $P_{\rm rot}$ | $3.295 \pm 0.003$ | day | 3 |
| $v \sin i$ | 6 | km s$^{-1}$ | 4 |
| $\log_{10}(L_{\rm H\alpha}/L_{\rm bol})$ | $-4.85$ to $-4.60$ | dex | 5–8 |
| $\log_{10}(L_{\rm X}/L_{\rm bol})$ | $-3.52 \pm 0.17$ | dex | 9 |
| Radius | $0.117 \pm 0.004$ | $R_\odot$ | 2 |
| ⋯ | $0.121 \pm 0.003$ | $R_\odot$ | 10 |
| Mass | $0.080 \pm 0.007$ | $M_\odot$ | 2 |
| Density | $50.7^{+1.2}_{-2.2}$ | $\rho_\odot$ | 2 |
| Age | $7.6 \pm 2.2$ | Gyr | 10 |
| **Astrometric/Kinematic Parameters** | | | |
| $\alpha$ | 346.6250957 | deg | 11 |
| $\delta$ | −5.0428081 | deg | 11 |
| $\mu_\alpha$ | $+922.0 \pm 0.6$ | mas yr$^{-1}$ | 12 |
| $\mu_\delta$ | $-471.9 \pm 0.9$ | mas yr$^{-1}$ | 12 |
| $\pi$ | $80.1 \pm 1.2$ | mas | 12 |
| Distance | $12.49 \pm 0.18$ | pc | 12 |
| $v_r$ | $-51.688 \pm 0.014$ | km s$^{-1}$ | 4 |
| $U$ | $-43.8 \pm 0.7$ | km s$^{-1}$ | 10 |
| $V$ | $-66.3 \pm 0.5$ | km s$^{-1}$ | 10 |
| $W$ | $+11.0 \pm 0.3$ | km s$^{-1}$ | 10 |
| $S$[a] | $80.0 \pm 0.7$ | km s$^{-1}$ | 10 |
| **Photometric Parameters** | | | |
| $V$ | $18.75 \pm 0.03$ | mag | 13 |
| $R_C$ | $16.401 \pm 0.004$ | mag | 14 |
| $I_C$ | $13.966 \pm 0.002$ | mag | 14 |
| $J$ | $11.35 \pm 0.02$ | mag | 15 |
| $H$ | $10.72 \pm 0.02$ | mag | 15 |
| $K_s$ | $10.30 \pm 0.02$ | mag | 15 |
| $W1$ | $10.07 \pm 0.02$ | mag | 11 |
| $W2$ | $9.81 \pm 0.02$ | mag | 11 |
| $W3$ | $9.51 \pm 0.04$ | mag | 11 |
| $V - K_s$ | $+8.45 \pm 0.04$ | mag | 13, 15 |
| $M_V$ | $18.27 \pm 0.04$ | mag | 10 |
| $M_J$ | $10.87 \pm 0.04$ | mag | 10 |
| $M_{K_s}$ | $9.81 \pm 0.04$ | mag | 10 |

**Note.**
[a] Total speed relative to the Sun.
**References.** (1) Filippazzo et al. (2015), (2) Gillon et al. (2016), (3) Vida et al. (2017), (4) Barnes et al. (2014), (5) Gizis et al. (2000), (6) Reiners & Basri (2008), (7) Barnes et al. (2014), (8) Burgasser et al. (2015), (9) Wheatley et al. (2017) (10) This paper; (11) AllWISE epoch 2010.5589 (Wright et al. 2010); (12) Weinberger et al. (2016), (13) Winters et al. (2015), (14) Liebert & Gizis (2006), (15) 2MASS (Skrutskie et al. 2006).

Also shown on the CMD are recent isochrones of low-mass stars of solar composition from Baraffe et al. (2015) for ages of 0.2, 0.3, 0.5, 3, and 8 Gyr; and masses of 0.07, 0.08, and 0.09 $M_\odot$, spanning current mass estimates for TRAPPIST-1. These isochrones reproduce the empirical locus for late M dwarfs to an accuracy of ∼0.1–0.2 mag in $M_{Ks}$ or ∼0.2 mag in $(V - K_s)$ color, but not for the greater spread, which is likely due to metallicity scatter (López-Morales 2007). Binaries are relatively rare among late M dwarfs (∼10%–20%; Allen 2007; Kraus & Hillenbrand 2012) and most field stars will be older than the pre-main-sequence contraction timescale of hundreds of Myr.

TRAPPIST-1 lies $0.15 \pm 0.04$ mag above (brighter than) the empirical locus. This offset could be interpreted as TRAPPIST-1 being a 0.2–0.3 Gyr old, 0.07 $M_\odot$ brown dwarf. However, this interpretation would predict a density of 38 $\rho_\odot$ based on the Baraffe et al. (2015) models, which is much lower than the measured density from transit observations (see below). We can also rule out contamination from a stellar or substellar companion based on previous adaptive optics surveys (Bouy et al. 2003; Gizis et al. 2003; Siegler et al. 2003; Janson et al. 2012) and multi-epoch radial velocity studies (Tanner et al. 2012; Barnes et al. 2014).

Instead, the magnitude offset of TRAPPIST-1 is likely due to a slightly supersolar metallicity. The offset is similar to that of the M8 V standard VB 10 (aka GJ 752B), and both it and its M3 V companion, GJ 752A, are slightly metal-rich ([Fe/H] $= 0.09 \pm 0.12$ and $0.10 \pm 0.08$, respectively; Newton et al. 2014; Mann et al. 2015), which is consistent with the spectroscopic value for TRAPPIST-1 (Gillon et al. 2016). Alternately, attributing the 0.48 mag scatter in the absolute magnitudes of late M dwarfs entirely to metallicity scatter (∼0.2 dex) would imply a metallicity-absolute magnitude gradient of $\Delta[{\rm Fe/H}]/\Delta M_{Ks} \simeq -0.4$ dex mag$^{-1}$, with metal-rich stars being brighter. Under this interpretation, the −0.15 mag absolute magnitude offset for TRAPPIST-1 would be consistent with [Fe/H] $= +0.06$ dex, which is again consistent with the spectroscopic metallicity,

Unfortunately, current evolutionary models for the very lowest-mass stars and brown dwarfs are defined only for solar metallicities, preventing us from disentangling age and metallicity effects. Our CMD analysis therefore reinforces a supersolar metallicity for TRAPPIST-1, but cannot constrain its age.

### 2.2. Age Constraints from Stellar Density

Average stellar density, an observable from transit lightcurve analysis (Seager & Mallén-Ornelas 2003), provides an independent check on the evolutionary state of TRAPPIST-1. Figure 1 shows the predicted average densities for stars and brown dwarfs from the solar-metallicity evolutionary models of Burrows et al. (1997, 2001) and Baraffe et al. (2015) as a function of age, constrained to have the observed luminosity of TRAPPIST-1. At this luminosity, young, contracting substellar objects have densities that increase up to an age of approximately 500 Myr; beyond 1 Gyr (corresponding to hydrogen-burning low-mass stars), densities plateau. The Burrows et al. models predict densities 17% higher than the Baraffe et al. models, corresponding to radii that are 6% smaller. The average density of TRAPPIST-1 is on the rising portion of this trend, and intersects with the Burrows et al. and Baraffe et al. models at ages of 0.3 and 0.4 Gyr, respectively, corresponding to masses at the hydrogen-burning mass limit (0.071 $M_\odot$ and 0.079 $M_\odot$).

These comparisons again suggest that TRAPPIST-1 could be relatively young. However, two factors confound this interpretation. First, there are the previously noted metallicity effects. Among $-0.04 <$ [Fe/H] $< 0.12$ low-mass stars, López-Morales (2007) found that evolutionary models underpredict stellar radii by 10%–20%, which is a correction factor sufficient to bring the density plateaus of the Baraffe et al. and Burrows et al. models in line with the observed density of

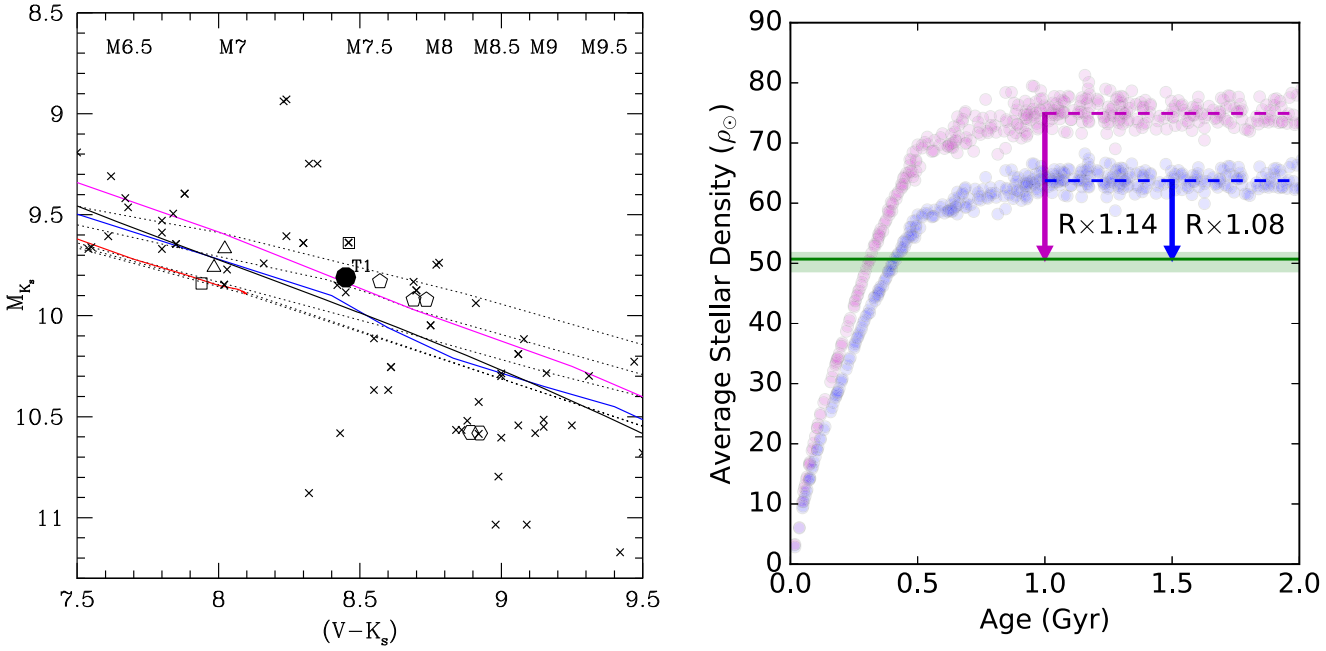


**Figure 1.** (Left) Color-absolute magnitude diagram ($M_{Ks}$ vs. $V - K_s$) for TRAPPIST-1; late M spectral standard stars from Kirkpatrick et al. (1991, 1997, 2010) and Henry et al. (2002, 2004), and late M field stars from Dieterich et al. (2014) and Winters et al. (2015). TRAPPIST-1 is plotted as a large filled circle; the spectral standards are indicated as open triangles (M7V), open squares (M7.5V), open pentagons (M8V), and open hexagons (M8.5V); all others as crosses. The color–magnitude locus for M dwarfs is plotted as a solid black line. Isochrones from Baraffe et al. (2015) for ages of 0.2, 0.3, 0.5, 3, and 8 Gyr (dashed lines, older isochrones toward the bottom); and masses of 0.07, 0.08, and 0.09 $M_\odot$ (from top to bottom, solid magenta, blue, and red lines, respectively) are also shown. Given the slow evolution of M dwarfs on the main sequence, the 3 and 8 Gyr isochrones are indistinguishable on the scale of the diagram. The approximate spectral types corresponding to $V - K_s$ color are listed along the top. (Right) Average density in solar units as a function of age based on the theoretical models of Burrows et al. (1997, 2001, black symbols) and Baraffe et al. (2015, blue symbols) for a luminosity $\log_{10} L/L_{\rm bol} = -3.28 \pm 0.03$. Values were selected by Monte Carlo sampling in age (uniform distribution) and luminosity (normal distribution). The average density measured for TRAPPIST-1 from Gillon et al. (2016), $50.7^{+1.2}_{-2.2}$ $\rho_\odot$, is indicated by the horizontal green line and region. The radius scale factors needed to "inflate" the models for ages >1 Gyr (dashed lines) to the average density of TRAPPIST-1 is indicated by the arrows.

TRAPPIST-1. Second, magnetic activity can also modulate the radii of low-mass stars and brown dwarfs (Chabrier et al. 2007; López-Morales 2007; Reiners et al. 2007; MacDonald & Mullan 2009; Mohanty et al. 2010). Empirical relations from Stassun et al. (2012) predict a modest effect: 0%–4% based on X-ray emission, and 4%–6% based on H$\alpha$ emission. However, theoretical models by Chabrier et al. (2007) show radii can range over 0.10–0.14 $R_\odot$ at $M = 0.08\,M_\odot$ for (black) spot surface coverage of up to 50%, which is more than sufficient to cover the difference between TRAPPIST-1's observed stellar density and models. *Kepler* data have confirmed the presence of cool, stable magnetic spots on TRAPPIST-1 (Luger et al. 2017; Vida et al. 2017), so these may play a role in radius inflation.

Given that both metallicity and magnetic activity likely play a role in setting the radius and average stellar density of TRAPPIST-1, current evolutionary models do not allow us to extract meaningful age constraints from this physical parameter.

### 2.3. Age Constraints from Lithium Depletion

Multiple studies have reported the absence of 6708 Å Li I absorption in the optical spectrum of TRAPPIST-1, indicating depletion of this element in its fully convective interior (Reiners & Basri 2009; Burgasser et al. 2015). As noted above, theoretical models of solar-metallicity stars and brown dwarfs more massive than 0.06 $M_\odot$ show full depletion within ∼200 Myr (Bildsten et al. 1997; Burke et al. 2004). Similarly, the Burrows et al. (1997, 2001) and Baraffe et al. (2015) evolutionary models predict a minimum age of 190 Myr for a 0.06 $M_\odot$ brown dwarf with the observed luminosity of TRAPPIST-1. These estimates provide a lower limit to TRAPPIST-1's age that is already incorporated into the age range proposed by Filippazzo et al. (2015).

### 2.4. Age Constraints from Surface Gravity Features

Low-resolution near-infrared spectra presented in Gillon et al. (2016) are generally consistent with the M8 dwarf spectral standard VB 10. However, there are some notable peculiarities, including weaker FeH absorption and a more triangular *H*-band peak (Figure 2). Application of the Allers & Liu (2013) surface gravity indices yield a gravity classification of INT-G for this source, suggesting a low surface gravity and young age (∼100–300 Myr). Moreover, comparison of its near-infrared spectrum to the entirety of the SpeX Prism Library (Burgasser 2014) uncovers an excellent match to the M7 dwarf 2MASS J2352050−110043 (Cruz et al. 2007; hereafter 2MASS J2352−1100), which is a source identified by Gagné et al. (2015a) and Aller et al. (2016) as a possible kinematic member of the ∼110 Myr AB Doradus association (Luhman et al. 2005; Barenfeld et al. 2013). These lines of evidence again suggest TRAPPIST-1 could be a young brown dwarf.

However, 2MASS J2352−1100 lacks Li I absorption, expected for a 110 Myr M8 dwarf; and it kinematic association with AB Doradus is based on proper motion and estimated distance alone, and may be spurious. TRAPPIST-1's kinematics firmly rule out membership in AB Doradus or any

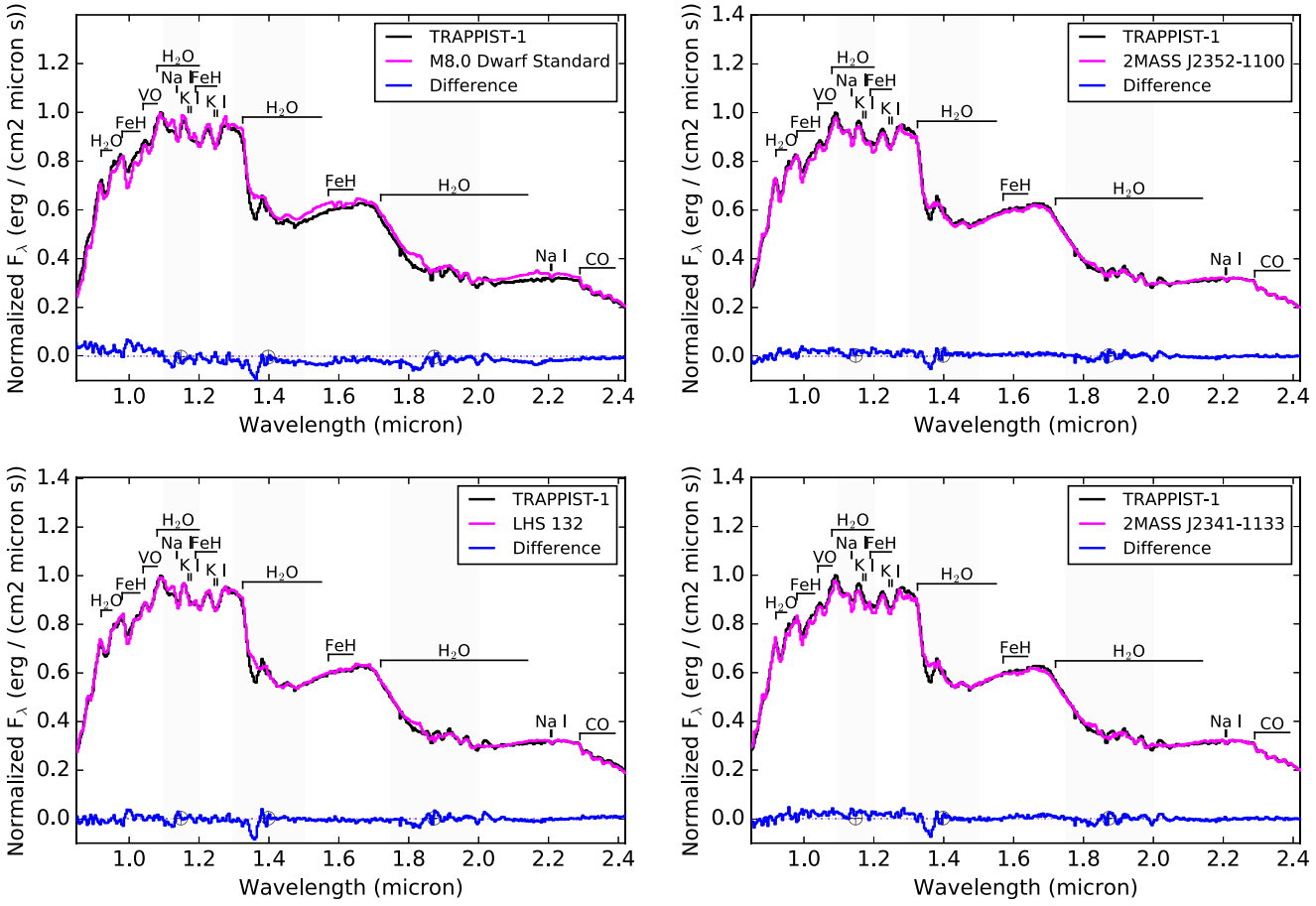


**Figure 2.** Comparison of the low-resolution near-infrared spectrum of TRAPPIST-1 (Gillon et al. 2016; black line) to equivalent data (red lines) for the M8 standard VB 10 (top left) and the M8 dwarfs 2MASS J2352050−110043 (top right), LHS 132 (bottom left), and 2MASS J2341286−113335 (bottom right). All comparison spectra are from Bardalez Gagliuffi et al. (2014), and are normalized to optimize agreement to the spectrum of TRAPPIST-1 outside telluric absorption bands (gray regions). Difference spectra are shown in blue. Absorption features attributable to Na I, K I, $H_2O$, CO, VO, and FeH are labeled.

nearby young moving group (Malo et al. 2013; Gagné et al. 2014); and neither TRAPPIST-1 nor 2MASS J2352−1100 exhibit the enhanced VO absorption generally seen in the spectra of low-gravity M and L dwarfs (Kirkpatrick et al. 2008; Cruz et al. 2009; Allers & Liu 2013). The near-infrared spectrum of TRAPPIST-1 is also a good match to those of the M8 dwarfs LP 938-71 and 2MASS J2341286−113335 (Figure 2), neither of which are reported to be unusually young or active (Cruz et al. 2007; Schmidt et al. 2007).

We conclude that the INT-G gravity classifications for both TRAPPIST-1 and 2MASS J2352−1100 are unrelated to youth, and may arise from other physical factors, as previously reported for the high velocity M6.5 2MASS J02530084+1652532 (aka Teegarden's star, $V_{\rm tan} = 93\,{\rm km\,s^{-1}}$; Teegarden et al. 2003; Henry et al. 2006; Gagné et al. 2015b) and the d/sdM7 metal-poor companion GJ 660.1B (Aganze et al. 2016). Given the apparent interplay between surface gravity and metallicity effects in index-based gravity diagnostics for late M dwarfs, we discount the INT-G classification as evidence of youth for TRAPPIST-1.

### 2.5. Age Constraints from Metallicity

While age–metallicity correlations are generally weak among stellar populations, the dispersion of stellar metallicities increases for populations older than a few Gyr, and median metallicity decreases for populations older than ≈10 Gyr (Edvardsson et al. 1993; Haywood et al. 2013; Bergemann et al. 2014). Hence, comparison of TRAPPIST-1's metallicity to population distributions can provide a statistical constraint on its age.

To quantify this diagnostic, we examined the age and metallicity distributions of stars drawn from the Spectroscopic Properties of Cool Stars (SPOCS; Valenti & Fischer 2005) and an updated analysis of the Geneva-Copenhagen Survey (GCS; Casagrande et al. 2011). In both samples, ages are inferred by comparison of CMDs to model isochrones (for GCS, we used the ages inferred from the Padova isochrones; Bertelli et al. 2008), while metallicities are determined from spectroscopic measurements in SPOCS and Strömgren photometry in GCS. For both samples, we selected $M \leqslant 1\,M_\odot$ stars with $-0.04 < {\rm [Fe/H]} < +0.12$ and parallactic distances within 30 pc, and constructed an age distribution by assuming a uniform likelihood for each star between the minimum and maximum ages (SPOCS) or 16% and 84% ($\pm 1\sigma$ for a normal distribution) Padova isochronal ages (GCS). These distributions are shown in Figure 3. In both samples, stars younger than 1–2 Gyr and older than 11–12 Gyr are relatively rare. The SPOCS age distribution peaks at young ages, which is enhanced by the metallicity constraint. The GCS age distribution is flat between 2 and 10 Gyr, with a slight preference toward younger ages with the metallicity constraint. While the maximum likelihood ages are quite different between these

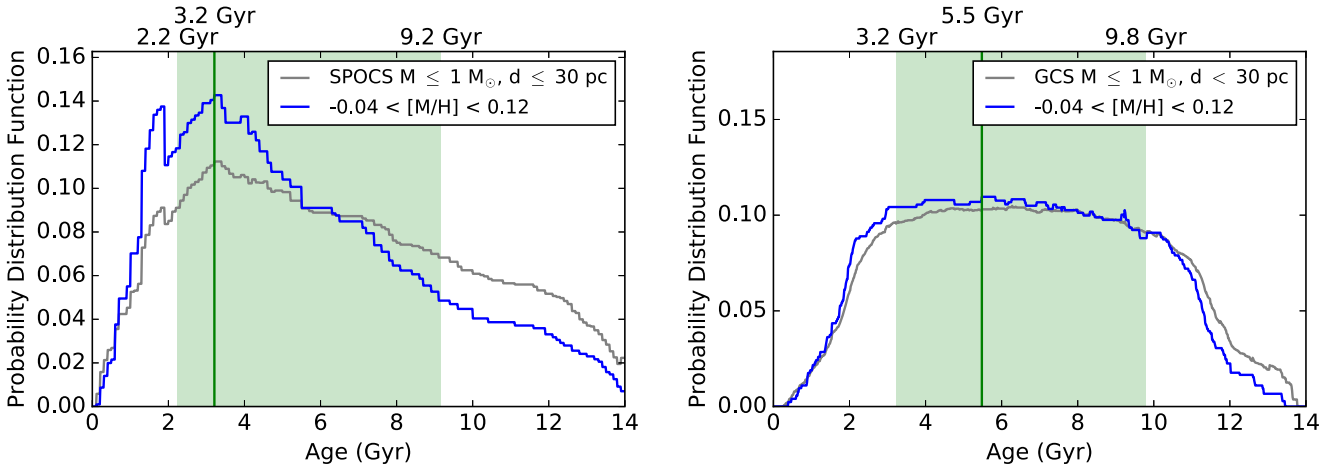


**Figure 3.** Age probability distribution functions for stars with $M \leqslant 1\,M_{\odot}$, $-0.04 < [\mathrm{Fe/H}] < +0.12$ and distances $\leqslant$30 pc in the SPOCS (left) and GCS (right) catalogs. Gray histograms are without the metallicity constraint; blue histograms are with the metallicity constraint. The solid vertical lines indicate the maximum likelihoods of the age distributions with all constraints, and the shaded green regions encompass the 16%–84% ($\pm 1\sigma$ for a normal distribution) probability ranges.

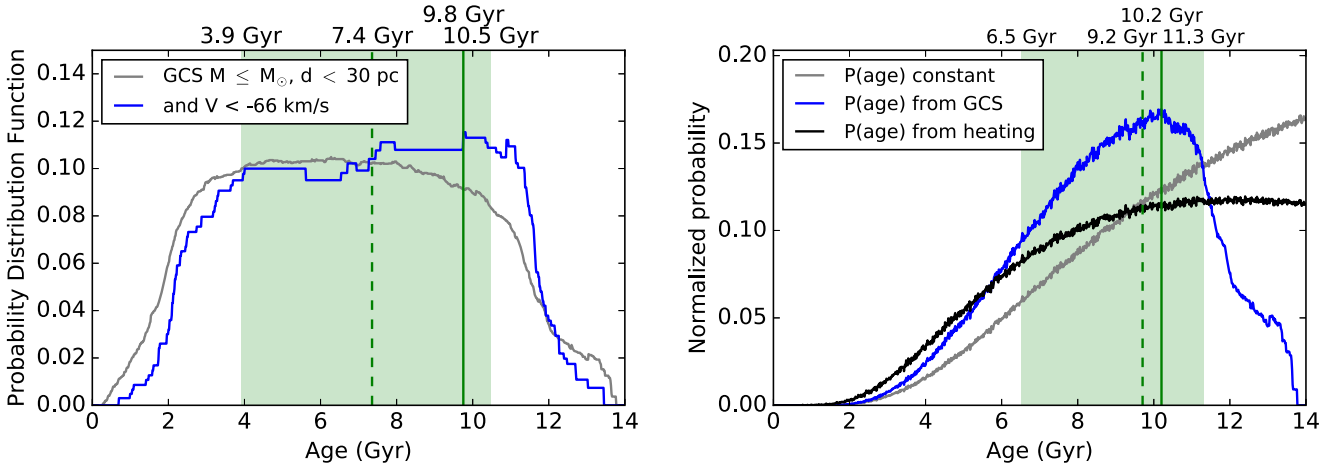


**Figure 4.** (Left) Distribution of ages of $M < 1\,M_{\odot}$ GCS stars (gray) compared to those with $V < -66$ km s$^{-1}$ (blue). (Right) Distribution of ages for a simulated population with *UVW* dispersions based on three different age priors: a constant prior (gray), a prior based on the GCS sample ($M \leqslant 1\,M_{\odot}$ and $d \leqslant 30$ pc; blue), and a prior based on a model for kinematic heating (black). In both panels, the solid vertical lines indicate the maximum likelihood values of the age distributions for the velocity-selected (left) and GCS prior (right) samples, the dashed vertical lines the medians, and the shaded green regions encompass the 16%–84% probability ranges.

samples, their distributions overlap, and we infer ages of $3.2^{+6.0}_{-1.0}$ Gyr for SPOCS and $5.5^{+3.7}_{-2.3}$ Gyr for GCS. As anticipated, the uncertainties are considerable and do little to reduce the overall uncertainty in the system's age.

### 2.6. Age Constraints from Kinematics

Reiners & Basri (2009) and Burgasser et al. (2015) previously reported statistically equivalent *UVW* kinematics for TRAPPIST-1 based on radial velocity and proper motion measurements, the latter study concluding that the star is a borderline thin/thick disk star based on the criteria of Bensby et al. (2003). We update this analysis using the more precise radial velocity reported in Barnes et al. (2014) and astrometry reported in Weinberger et al. (2016). The corresponding heliocentric *UVW* velocities are given in Table 1. Adopting the Local Standard of Rest (LSR) correction of Dehnen & Binney (1998) used by Bensby et al. (2003), $UVW_{\odot} = [+10.00, +5.25, +7.17]$, we find probabilities of kinematic association $P(\mathrm{thin}) = 81\%$, $P(\mathrm{thick}) = 19\%$, and $P(\mathrm{halo}) < 0.1\%$. With $P(\mathrm{thick})/P(\mathrm{thin}) = 0.23$, this star remains a borderline thin/thick disk star by the Bensby et al. (2003) criteria.

To derive a quantitative estimate of TRAPPIST-1's kinematic age, we took advantage of the fact that the *V*-velocity asymmetric drift of stellar populations increases over time as the velocity scatter increases ($V_a \propto \sigma_U^2$; Strömberg 1924). We again used the GCS sample and examined the age distribution of stars with negative *V* velocities like TRAPPIST-1. Figure 4 shows the same mass- and distance-constrained distribution as Figure 3, but with the additional constraint that $V < V_{T1} = -66$ km s$^{-1}$. In this case we see a tilt toward older ages, with a maximum likelihood value of 9.8 Gyr, albeit with a wide uncertainty range (3.9–10.5 Gyr). We find a similar distribution (albeit with a very small sample) when a metallicity constraint was also applied to the GCS sample.

As a second approach, we applied a Bayesian method to solve for the probability distribution function of a star's age given its UVW velocities:

$$P(\mathrm{age}|\mathrm{UVW}) \propto P(\mathrm{UVW}|\mathrm{age})P(\mathrm{age}). \quad (2)$$

Here, $P$(age) is the a priori distribution of stellar ages while $P$(UVW|age) is the distribution of stellar UVW velocities as they evolve over time. We considered three different age priors in our analysis: a constant age distribution (the constant star formation rate) up to 12 Gyr; the age distribution of GCS stars with $M \leqslant 1\,M_\odot$ and $d \leqslant 30$ pc without constraints on metallicity or $V$-velocity; and a constant age distribution with an additional "heating" term modeled after Aumer & Binney (2009) that deweights older populations that spend less time in the immediate solar neighborhood,

$$\ln P \propto -\frac{\Delta\Phi(Z)}{\sigma_W(t)^2}. \quad (3)$$

Here, $\Delta\Phi(Z)$ is the vertical gravitational potential difference from the mid-plane to a Galactic height $Z$, taken to be 50 pc; and $\sigma_W(t)$ is the vertical velocity dispersion over time $t$ in Gyr, calculated as

$$\sigma_W(t) = 8.388(t + 0.01)^{0.445}\ \mathrm{km\ s^{-1}} \quad (4)$$

(Aumer & Binney 2009). For the Galactic potential, we used the four-component disk, halo, and bulge model of Barros et al. (2016) at a Galactic radius of 8 kpc. UVW velocities as a function of age were drawn using the age-dispersion relations of Aumer & Binney (2009), including an asymmetric drift term $V_a = -\frac{\sigma_U^2}{74\ \mathrm{km\ s^{-1}}}$. We drew $10^7$ stars at each simulated time step and computed the fraction of draws as a function of age whose UVW velocities were within $5\sigma$ of those of TRAPPIST-1.

Figure 4 shows the resulting distribution of stellar ages for our three age priors. All are strongly skewed toward older ages, with maximum likelihood values ranging from 10.2 Gyr (GCS) to 12 Gyr (constant). The GCS and heating model priors produce similar distributions within 11 Gyr, the former dropping off rapidly beyond this in accord with the underlying sample age distribution. Using the median values as best estimates, we infer ages of $9.2^{+1.1}_{-2.7}$ Gyr and $8.7^{+2.3}_{-2.9}$ Gyr for the GCS and heating model priors, which are on the high end but consistent with the other age diagnostics.

### 2.7. Age Constraints from Rotation

While the timescales for rotation spin down and activity decline for ultracool dwarfs become exceedingly long compared to more massive stars (West et al. 2008; Irwin et al. 2011), there is evidence that both properties do evolve in a measurable way (e.g., Burgasser et al. 2015). Early analysis of TRAPPIST-1 has suggested that its 3.295 day rotation period is average for late-type M dwarfs, suggesting a "middle-age" star (3–8 Gyr from Luger et al. 2017).

To quantify this, we compared the rotation period of TRAPPIST-1 to those of mid- and late M dwarfs observed through the MEarth program (Nutzman & Charbonneau 2008) as reported in Newton et al. (2016). Selecting subsamples of stars with significant periodic variability ($A/\sigma_A > 2$) in 0.02 $M_\odot$ bins over masses of 0.07–0.18 $M_\odot$, we computed the fraction of each subsample that had periods longer than TRAPPIST-1. Figure 5 shows the resulting trend, illustrating that roughly 60% of the stars observed in this study were slower rotators, which suggests that they are older. If we assume (simplistically) that rotation declines monotonically over time, and use the GCS sample as an age prior, this analysis would suggest an age of ∼4–5 Gyr for TRAPPIST-1, depending on the assumed age of the Milky Way.

However, the rotation periods of very low-mass stars at late ages are highly sensitive to initial conditions and the mechanism for angular momentum loss. Figure 5 shows the evolution of rotation period for a 0.08 $M_\odot$ star following the angular momentum loss rate prescription of Chaboyer et al. (1995) and Krishnamurthi et al. (1997) as previously applied to low-mass stars (e.g., Bouvier et al. 1997; Reiners & Basri 2008; Irwin et al. 2011). We assumed a critical (or saturation) rotation rate $\omega_{\rm crit} = \omega_{\rm crit,\odot}\frac{\tau_\odot}{\tau} = 1.86\omega_\odot$, where $\omega_{\rm crit,\odot} = 10\omega_\odot$ and $\tau$ is the convective overturn time assumed proportional to $M^{-2/3}$ (Reiners & Basri 2008). We used the time-dependent radii for an $M = 0.08\ M_\odot$ from the models of Baraffe et al. (2003). We considered both "slow" and "fast" prescriptions for spin down[4] from Irwin et al. (2011), as well as a range of initial rotation velocities at ∼20–50 Myr of 20–100 $\omega_\odot$, based on measurements for $M < 0.35\ M_\odot$ stars in NGC 2547 reported in the same study. As shown in Figure 5, different angular momentum loss prescriptions produce widely dispersed rotation periods beyond 300 Myr, spanning nearly three orders of magnitude by 10 Gyr. This range is well-matched to the range of observed rotation periods for significantly variable 0.06–0.10 $M_\odot$ stars in the sample of Newton et al. (2016), which span 0.11–364 days. TRAPPIST-1's rotation period resides between the slow and fast evolutionary tracks. Since neither the specific mechanism of spin down nor the initial rotation rate are known for this source, at best we can conclude that TRAPPIST-1 is likely older than 300 Myr, the age at which the "fast" track periods exceed 3.3 days.

### 2.8. Age Constraints from Activity

Low-mass stars show clear age-activity correlations related to the spin down of stars and reduction of rotationally driven magnetic dynamos (Skumanich 1972; Feigelson & Lawson 2004; Covey et al. 2008). As spin-down timescales increase for the lowest-mass stars, saturated magnetic emission can persist for even slowly rotating stars ($P < 86$ day) with little correlation between the incidence of emission and rotation period (West et al. 2008, 2015). However, there is evidence for a correlation between the strength of H$\alpha$ emission and "stratigraphic" age (the distance from the Galactic plane) that continues through the end of the M dwarf sequence.

Persistent H$\alpha$ emission from TRAPPIST-1 is weaker than emission in over half of the active late M dwarfs near the Sun (Figure 6), suggesting an age in the upper half of this sample. This comparison stands in contrast to claims that TRAPPIST-1 is "highly active," which suggests youth (e.g., Bourrier et al. 2017; Vida et al. 2017). The perception that TRAPPIST-1 is highly active is also related to its flaring emission, specifically the detection of a supersolar flare in its $K2$ lightcurve, with an integrated energy $E = 10^{33}$ erg (Vida et al. 2017). Again, context is essential. M dwarfs typically have higher optical and infrared flare rates and flare energies than solar-type stars (Davenport et al. 2012), and TRAPPIST-1's flare duty cycle during the $K2$ monitoring period, ≈0.1%[5] as reported by Vida

[4] In the notation of Chaboyer et al. (1995) these are $K_{\rm slow} = 1.20 \times 10^{45}$ g cm$^2$ s $= 1.25 \times 10^{-10}\ M_\odot\ R_\odot^2$ s and $K_{\rm fast} = 1.12 \times 10^{47}$ g cm$^2$ s $= 1.16 \times 10^{-8}\ M_\odot\ R_\odot^2$ s, respectively.

[5] Based on a typical flare timescale of 1–2 minute = 0.02–0.03 hr and the median time between flares 28.1 hr.

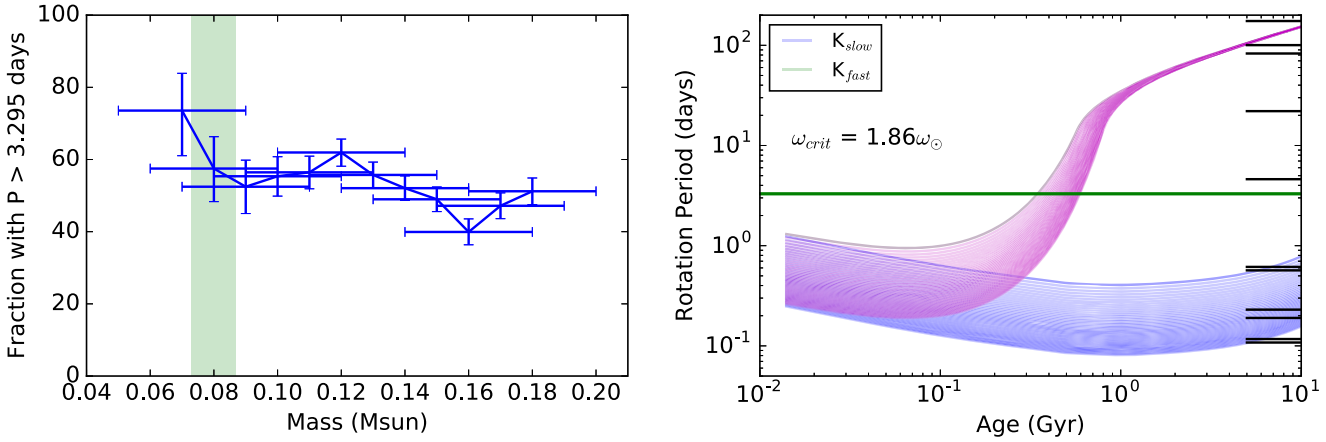


**Figure 5.** (Left) Fraction of sources in the Newton et al. (2016) sample with rotation periods greater than 3.295 days as a function of mass. Horizontal error bars indicate the sample bin size, vertical error bars the binomial sampling uncertainties. For the mass estimate of TRAPPIST-1, just over half of the sample spins slower, suggesting this source is roughly "middle-age" for an ultracool M dwarf. (Right) Angular momentum evolution for a 0.08 $M_\odot$ star based on "slow" (blue lines) and "fast" (green lines) momentum loss following the prescription of Chaboyer et al. (1995) and Irwin et al. (2011). The various lines sample initial rotation rates of 20–100 $\omega_\odot$. The observed rotation period of TRAPPIST-1 is indicated by the solid black line; the red marks to the right of the panel indicate rotation periods measured for 0.06–0.10 $M_\odot$ stars by Newton et al. (2016).

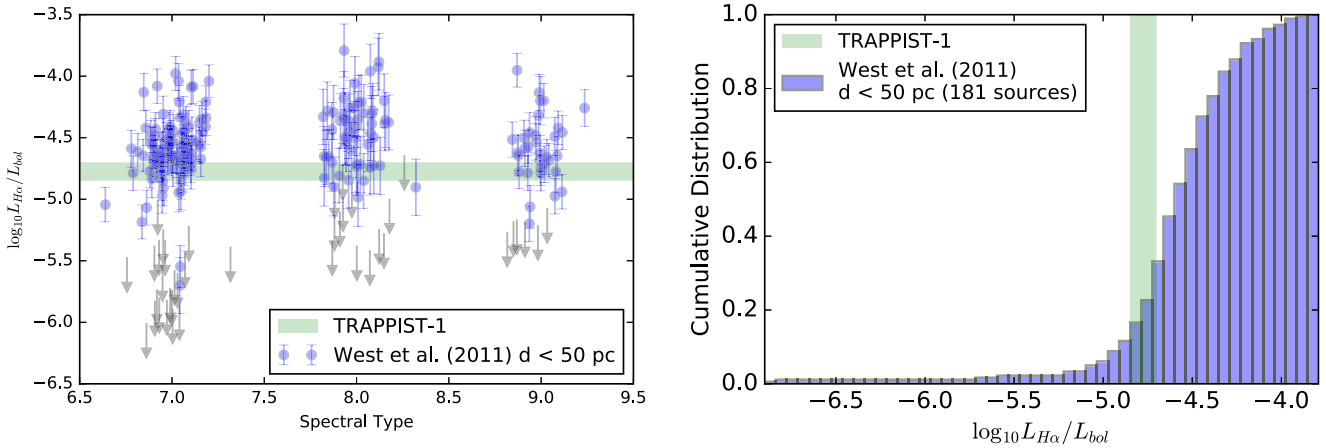


**Figure 6.** (Left) Measurements of $\log_{10} L_{H\alpha}/L_{bol}$ for 239 M7–M9 dwarfs with 50 pc with SDSS spectra as reported by West et al. (2011, circles and arrows) compared to the range of values reported for TRAPPIST-1 (green region; Table 1). Circles with error bars are sources with significant detections (H$\alpha$ emission peak more than three times the continuum noise); downward arrows are upper limits. Points are randomly offset along the x-axis to aid in visualization. (Right) Cumulative distribution of significant $\log_{10} L_{H\alpha}/L_{bol}$ measurements for the SDSS sample, again compared to the range of measurements for TRAPPIST-1. This star is less active than over half of the nearby M7–M9 dwarfs.

et al. (2017), is more than an order of magnitude below the $3 \pm 1\%$ inferred for M7–M9 dwarfs by Hilton et al. (2010). The cumulative flare frequency distribution for TRAPPIST-1 as a function of energy, also reported in Vida et al. (2017), is similarly depressed by a factor of $\approx$4 compared to other M6-M8 dwarfs (Hilton 2011; Gizis et al. 2017a). Finally, the *K2* flare, while dramatic, is not unique; Gizis et al. (2017b) report an $E > 4 \times 10^{33}$ erg flare from an L0 dwarf observed with *K2*, and Schmidt et al. (2014, 2016) have reported $E > 10^{34}$ erg flares from M8 and L1 dwarfs detected in the All-Sky Automated Survey for Supernovae survey (Shappee et al. 2014).

Taken together, these activity metrics suggest TRAPPIST-1 is older than the typical late M dwarf in the solar neighborhood, but remains an active star. Given the lack of empirical calibrations for age/activity among the latest M dwarfs, we are unable to more specifically quantify TRAPPIST-1's age from these measures.

## 3. Discussion

Combining our age probability distribution functions from metallicity and kinematics, and lower limits from the absence of lithium absorption and measured rotation period, we deduce a concordance age of $7.6 \pm 2.2$ Gyr for TRAPPIST-1 (Figure 7). This is inconsistent with some of the qualitative estimates reported in the literature (e.g., "relatively young," Bourrier et al. 2017; "young," O'Malley-James & Kaltenegger 2017), and is on the high end of the 3–8 Gyr age adopted by Luger et al. (2017). This older age has important implications on both the stability and habitability of its orbiting planets.

In terms of stability, N-body simulations presented in Gillon et al. (2017) showed the planetary system to be consistently unstable on timescales <0.5 Myr, with only an 8% change of surviving 1 Gyr. This is refuted by the much older age we infer for the TRAPPIST-1 star. More recent simulations show that the resonant configuration of these planets is stable through disk migration on timescales of 50 Myr ($10^{10}$ orbits), with or

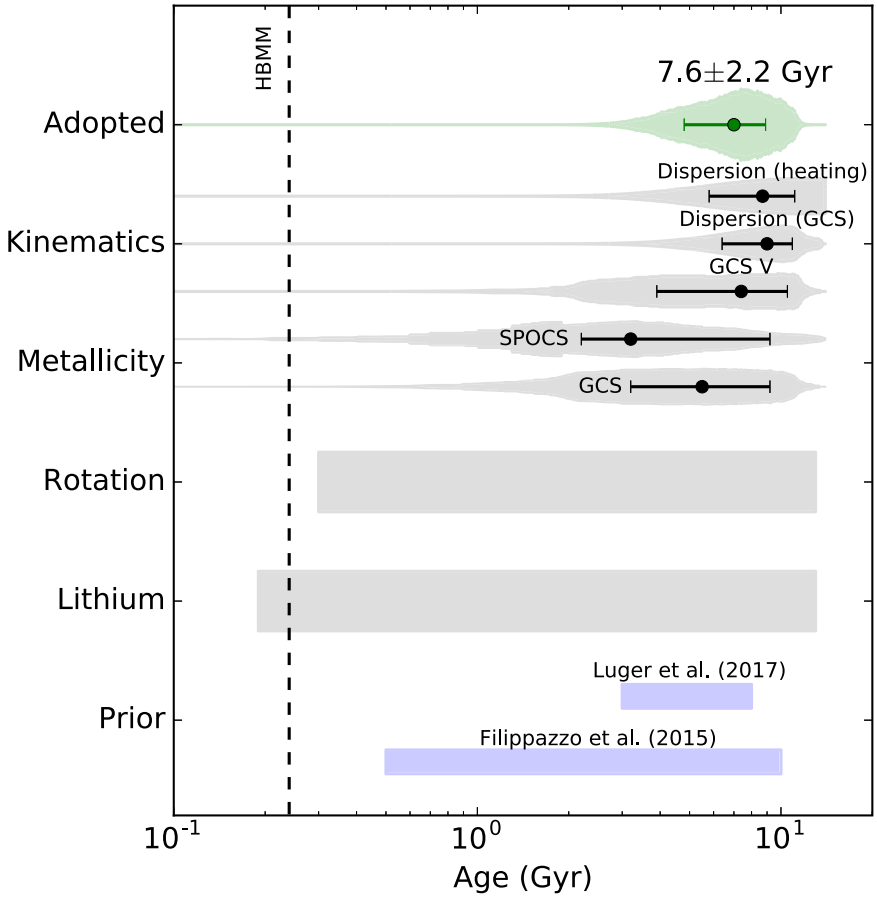


**Figure 7.** Summary of age estimates for TRAPPIST-1, from bottom to top: the original age range from Filippazzo et al. (2015); the estimated age range form Luger et al. (2017); the lower limit based on absence of Li I absorption; the lower limit based on rotation period; age probability distribution functions for GCS and SPOCS stars with similar metallicities; the age probability distribution function for GCS stars with $V \leqslant V_{T1}$; kinematic dispersion simulations with age priors based on the GCS sample (lower) and heating losses (upper); and our concordance age estimate. No viable age constraints could be made from color–magnitude diagram, average density, surface gravity, or magnetic activity diagnostics. Throughout, symbols with error bars indicate the maximum likelihood and 16%–84% probability ranges, while the shaded regions map the underlying probability distribution functions.

without eccentricity dampening. This system appears to have persisted for over 5 Gyr, despite dynamical interactions that are readily detectable through transit timing variations (Gillon et al. 2017; Wang et al. 2017), suggesting that the resonant configuration is indeed quite stable.

In terms of habitability, despite TRAPPIST-1's modest emission as compared to other late M dwarfs, the radiation and particle environment is still extreme as compared to the Earth (Bolmont et al. 2017; Garraffo et al. 2017; Wheatley et al. 2017). Based on current estimates of XUV-driven mass loss, the high energy emission of TRAPPIST-1 is likely sufficient to have evaporated the equivalent water mass as the Earth's oceans from each of the TRAPPIST-1 planets, except *g* and *h,* over the system's lifetime (Bolmont et al. 2017; Bourrier et al. 2017). Moreover, the stripping of atmospheres and oceans may be enhanced by direct interaction between stellar and planetary magnetic field lines, which could funnel stellar wind particles directly to the planets' surfaces (Garraffo et al. 2016, 2017). On the other hand, current estimates of the planets' densities are generally below Earth's average density (Gillon et al. 2017; Wang et al. 2017), suggesting volatile-rich worlds that may have ample reservoirs of water, while ocean evaporation and hydrogen loss could result in an oxygen- and ozone-rich atmosphere that could shield the surface from high UV fluxes (Luger & Barnes 2015; O'Malley-James & Kaltenegger 2017). Transit spectroscopy measurements of the atmospheres of these planets are currently insufficient to detect the signatures of all but the lightest elements (de Wit et al. 2016), but the *James Webb Space Telescope* should have the sensitivity to detect Earth-like atmospheres around these plants, if they exist (Barstow & Irwin 2016).

Finally, we note that agreement between the observed luminosity, average stellar density, and evolutionary models can be achieved if the star's radius is modestly inflated relative to model predictions. Our analysis indicates that a radius of $0.121 \pm 0.003\ R_{\odot}$ is needed to bring both Burrows et al. (1997, 2001) and Baraffe et al. (2015) evolutionary models in line with the observed properties of TRAPPIST-1. This radius is formally consistent with the value adopted in Gillon et al. (2016), and represents a modest 3% increase in planetary radii and 11% decrease in inferred planetary densities, which is within current uncertainties (Gillon et al. 2017; Wang et al. 2017).

The authors acknowledge useful discussions with Eric Agol, Vincent Bourrier, Amaury Triaud, and Valerie van Grootel that aided in the preparation of the manuscript. The authors also thank the Hon. John Culberson of Texas's 7th congressional district, US House of Representatives, for asking about the age of TRAPPIST-1 during his visit to Jet Propulsion Laboratory in

2017 February, which spurred the writing of this paper. We thank our anonymous referee for their prompt review of the original manuscript. E.E.M. acknowledges the NASA NExSS program for support. A.J.B. acknowledges funding support from the National Science Foundation under award No. AST-1517177. Part of this research was carried out at the Jet Propulsion Laboratory, California Institute of Technology, under a contract with the National Aeronautics and Space Administration. This document has been approved for unlimited release (CL#17-3280). This material is based upon work supported by the National Aeronautics and Space Administration under Grant No. NNX16AF47G issued through the Astrophysics Data Analysis Program This research has made use of the SIMBAD database, operated at CDS, Strasbourg, France; NASA's Astrophysics Data System Bibliographic Services; the M, L, T, and Y dwarf compendium housed at http://DwarfArchives.org; and the Spex Prism Libraries at http://www.browndwarfs.org/spexprism. This publication makes use of data products from the Wide-field Infrared Survey Explorer, which is a joint project of the University of California, Los Angeles, and the Jet Propulsion Laboratory/California Institute of Technology, and NEOWISE, which is a project of the Jet Propulsion Laboratory/California Institute of Technology. WISE and NEOWISE are funded by NASA.

*Software:* astropy (Astropy Collaboration et al. 2013), SPLAT (Burgasser 2014).

## ORCID iDs

Adam J. Burgasser https://orcid.org/0000-0002-6523-9536
Eric E. Mamajek https://orcid.org/0000-0003-2008-1488

## References

Aganze, C., Burgasser, A. J., Faherty, J. K., et al. 2016, AJ, 151, 46
Allen, P. R. 2007, ApJ, 668, 492
Aller, K. M., Liu, M. C., Magnier, E. A., et al. 2016, ApJ, 821, 120
Allers, K. N., & Liu, M. C. 2013, ApJ, 772, 79
Astropy Collaboration, Robitaille, T. P., Tollerud, E. J., et al. 2013, A&A, 558, A33
Aumer, M., & Binney, J. J. 2009, MNRAS, 397, 1286
Baraffe, I., Chabrier, G., Barman, T. S., Allard, F., & Hauschildt, P. H. 2003, A&A, 402, 701
Baraffe, I., Homeier, D., Allard, F., & Chabrier, G. 2015, A&A, 577, A42
Bardalez Gagliuffi, D. C., Burgasser, A. J., Gelino, C. R., et al. 2014, ApJ, 794, 143
Barenfeld, S. A., Bubar, E. J., Mamajek, E. E., & Young, P. A. 2013, ApJ, 766, 6
Barnes, J. R., Jenkins, J. S., Jones, H. R. A., et al. 2014, MNRAS, 439, 3094
Barros, D. A., Lépine, J. R. D., & Dias, W. S. 2016, A&A, 593, A108
Barstow, J. K., & Irwin, P. G. J. 2016, MNRAS, 461, L92
Bensby, T., Feltzing, S., & Lundström, I. 2003, A&A, 410, 527
Bergemann, M., Ruchti, G. R., Serenelli, A., et al. 2014, A&A, 565, A89
Bertelli, G., Girardi, L., Marigo, P., & Nasi, E. 2008, A&A, 484, 815
Bildsten, L., Brown, E. F., Matzner, C. D., & Ushomirsky, G. 1997, ApJ, 482, 442
Bolmont, E., Selsis, F., Owen, J. E., et al. 2017, MNRAS, 464, 3728
Bourrier, V., Ehrenreich, D., Wheatley, P. J., et al. 2017, A&A, 599, L3
Bouvier, J., Forestini, M., & Allain, S. 1997, A&A, 326, 1023
Bouy, H., Brandner, W., Martín, E. L., et al. 2003, AJ, 126, 1526
Burgasser, A. J., Logsdon, S. E., Gagné, J., et al. 2015, ApJS, 220, 18
Burgasser, A. J. 2014, in Astronomical Society of India Conf. Ser. 11, International Workshop on Stellar Spectral Libraries, ed. H. P. Singh, P. Prugniel, & I. Vauglin (Bangalore: ASI), 7
Burke, C. J., Pinsonneault, M. H., & Sills, A. 2004, ApJ, 604, 272
Burrows, A., Hubbard, W. B., Lunine, J. I., & Liebert, J. 2001, RvMP, 73, 719
Burrows, A., Marley, M., Hubbard, W. B., et al. 1997, ApJ, 491, 856
Casagrande, L., Schönrich, R., Asplund, M., et al. 2011, A&A, 530, A138
Chaboyer, B., Demarque, P., & Pinsonneault, M. H. 1995, ApJ, 441, 865
Chabrier, G., Gallardo, J., & Baraffe, I. 2007, A&A, 472, L17
Covey, K. R., Agüeros, M. A., Green, P. J., et al. 2008, ApJS, 178, 339
Cruz, K. L., Kirkpatrick, J. D., & Burgasser, A. J. 2009, AJ, 137, 3345
Cruz, K. L., Reid, I. N., Kirkpatrick, J. D., et al. 2007, AJ, 133, 439
Davenport, J. R. A., Becker, A. C., Kowalski, A. F., et al. 2012, ApJ, 748, 58
Dehnen, W., & Binney, J. J. 1998, MNRAS, 298, 387
de Wit, J., Wakeford, H. R., Gillon, M., et al. 2016, Natur, 537, 69
Dieterich, S. B., Henry, T. J., Jao, W.-C., et al. 2014, AJ, 147, 94
Edvardsson, B., Andersen, J., Gustafsson, B., et al. 1993, A&A, 275, 101
Feigelson, E. D., & Lawson, W. A. 2004, ApJ, 614, 267
Filippazzo, J. C., Rice, E. L., Faherty, J., et al. 2015, ApJ, 810, 158
Gagné, J., Faherty, J. K., Cruz, K. L., et al. 2015b, ApJS, 219, 33
Gagné, J., Lafrenière, D., Doyon, R., Malo, L., & Artigau, É 2014, ApJ, 783, 121
Gagné, J., Lafrenière, D., Doyon, R., Malo, L., & Artigau, É 2015a, ApJ, 798, 73
Garraffo, C., Drake, J. J., & Cohen, O. 2016, ApJL, 833, L4
Garraffo, C., Drake, J. J., Cohen, O., Alvarado-Gomez, J. D., & Moshou, S. P. 2017, ApJL, 843, L33
Gillon, M., Jehin, E., Lederer, S. M., et al. 2016, Natur, 533, 221
Gillon, M., Triaud, A. H. M. J., Demory, B.-O., et al. 2017, Natur, 542, 456
Gizis, J. E., Monet, D. G., Reid, I. N., et al. 2000, AJ, 120, 1085
Gizis, J. E., Paudel, R. R., Mullan, D., et al. 2017a, arXiv:1703.08745
Gizis, J. E., Paudel, R. R., Schmidt, S. J., Williams, P. K. G., & Burgasser, A. J. 2017b, ApJ, 838, 22
Gizis, J. E., Reid, I. N., Knapp, G. R., et al. 2003, AJ, 125, 3302
Haywood, M., Di Matteo, P., Lehnert, M. D., Katz, D., & Gómez, A. 2013, A&A, 560, A109
Henry, T. J., Jao, W.-C., Subasavage, J. P., et al. 2006, AJ, 132, 2360
Henry, T. J., Subasavage, J. P., Brown, M. A., et al. 2004, AJ, 128, 2460
Henry, T. J., Walkowicz, L. M., Barto, T. C., & Golimowski, D. A. 2002, AJ, 123, 2002
Hilton, E. J. 2011, PhD thesis, Univ. Washington
Hilton, E. J., West, A. A., Hawley, S. L., & Kowalski, A. F. 2010, AJ, 140, 1402
Irwin, J., Berta, Z. K., Burke, C. J., et al. 2011, ApJ, 727, 56
Janson, M., Hormuth, F., Bergfors, C., et al. 2012, ApJ, 754, 44
Kirkpatrick, J. D., Beichman, C. A., & Skrutskie, M. F. 1997, ApJ, 476, 311
Kirkpatrick, J. D., Cruz, K. L., Barman, T. S., et al. 2008, ApJ, 689, 1295
Kirkpatrick, J. D., Henry, T. J., & McCarthy, D. W., Jr. 1991, ApJS, 77, 417
Kirkpatrick, J. D., Looper, D. L., Burgasser, A. J., et al. 2010, ApJS, 190, 100
Kraus, A. L., & Hillenbrand, L. A. 2012, ApJ, 757, 141
Krishnamurthi, A., Pinsonneault, M. H., Barnes, S., & Sofia, S. 1997, ApJ, 480, 303
Leggett, S. K. 1992, ApJS, 82, 351
Liebert, J., & Gizis, J. E. 2006, PASP, 118, 659
López-Morales, M. 2007, ApJ, 660, 732
Luger, R., & Barnes, R. 2015, AsBio, 15, 119
Luger, R., Sestovic, M., Kruse, E., et al. 2017, arXiv:1703.04166
Luhman, K. L., Stauffer, J. R., & Mamajek, E. E. 2005, ApJL, 628, L69
MacDonald, J., & Mullan, D. J. 2009, ApJ, 700, 387
Malo, L., Doyon, R., Lafrenière, D., et al. 2013, ApJ, 762, 88
Mann, A. W., Feiden, G. A., Gaidos, E., Boyajian, T., & von Braun, K. 2015, ApJ, 804, 64
Mohanty, S., Stassun, K. G., & Doppmann, G. W. 2010, ApJ, 722, 1138
Newton, E. R., Charbonneau, D., Irwin, J., et al. 2014, AJ, 147, 20
Newton, E. R., Irwin, J., Charbonneau, D., et al. 2016, ApJ, 821, 93
Nutzman, P., & Charbonneau, D. 2008, PASP, 120, 317
O'Malley-James, J. T., & Kaltenegger, L. 2017, MNRAS, 469, L26
Reiners, A., & Basri, G. 2008, ApJ, 684, 1390
Reiners, A., & Basri, G. 2009, ApJ, 705, 1416
Reiners, A., Seifahrt, A., Stassun, K. G., Melo, C., & Mathieu, R. D. 2007, ApJL, 671, L149
Schmidt, S. J., Cruz, K. L., Bongiorno, B. J., Liebert, J., & Reid, I. N. 2007, AJ, 133, 2258
Schmidt, S. J., Prieto, J. L., Stanek, K. Z., et al. 2014, ApJL, 781, L24
Schmidt, S. J., Shappee, B. J., Gagné, J., et al. 2016, ApJL, 828, L22
Seager, S., & Mallén-Ornelas, G. 2003, ApJ, 585, 1038
Sestito, P., & Randich, S. 2005, A&A, 442, 615
Shappee, B. J., Prieto, J. L., Grupe, D., et al. 2014, ApJ, 788, 48
Siegler, N., Close, L. M., Mamajek, E. E., & Freed, M. 2003, ApJ, 598, 1265
Skrutskie, M. F., Cutri, R. M., Stiening, R., et al. 2006, AJ, 131, 1163
Skumanich, A. 1972, ApJ, 171, 565

Soderblom, D. R. 2010, ARA&A, 48, 581
Stassun, K. G., Kratter, K. M., Scholz, A., & Dupuy, T. J. 2012, ApJ, 756, 47
Stauffer, J. R., Schultz, G., & Kirkpatrick, J. D. 1998, ApJL, 499, L199
Strömberg, G. 1924, ApJ, 59, 228
Tanner, A., White, R., Bailey, J., et al. 2012, ApJS, 203, 10
Teegarden, B. J., Pravdo, S. H., Hicks, M., et al. 2003, ApJL, 589, L51
Valenti, J. A., & Fischer, D. A. 2005, ApJS, 159, 141
Vida, K., Kővári, Z., Pál, A., Oláh, K., & Kriskovics, L. 2017, arXiv:1703.10130
Wang, S., Wu, D.-H., Barclay, T., & Laughlin, G. P. 2017, arXiv:1704.04290
Weinberger, A. J., Boss, A. P., Keiser, S. A., et al. 2016, AJ, 152, 24
West, A. A., Hawley, S. L., Bochanski, J. J., et al. 2008, AJ, 135, 785
West, A. A., Morgan, D. P., Bochanski, J. J., et al. 2011, AJ, 141, 97
West, A. A., Weisenburger, K. L., Irwin, J., et al. 2015, ApJ, 812, 3
Wheatley, P. J., Louden, T., Bourrier, V., Ehrenreich, D., & Gillon, M. 2017, MNRAS, 465, L74
Winters, J. G., Henry, T. J., Lurie, J. C., et al. 2015, AJ, 149, 5
Wright, E. L., Eisenhardt, P. R. M., Mainzer, A., et al. 2010, AJ, 140, 1868